INCORPORATION OF BENZOTHIAZOLE AND PYRIMIDINE MOIETIES ON NAPTHOL PLATFORM FOR THEIR SENSING PROPERTIES

A

Thesis submitted

In the partial fulfilment of the requirement for the degree of

MASTERS OF SCIENCE

IN

CHEMISTRY

Submitted By

CHARU GOYAL

(301602011)

UNDER THE SUPERVISION OF

Dr. VIJAY LUXAMI

(Associate Professor)

SCHOOL OF CHEMISTRY AND BIOCHEMISTRY,

THAPAR INSTITUTE OF ENGINEERING AND TECHNOLOGY,

PATIALA 147004

2018

CERTIFICATE

I hereby declare that the thesis entitled "INCORPORATION OF BENZOTHIAZOLE AND PYRIMIDINE MOIETIES ON NAPTHOL PLATFORM FOR THEIR SENSING PROPERTIES" is an authentic record of my work carried out as requirements for the award of degree of **Masters of Science** in **Chemistry** at, **Thapar Institute of Engineering and Technology, Patiala** under the supervision of **Dr. Vijay Luxami**, Associate Professor, School of Chemistry and Biochemistry, Thapar Institute of Engineering and Technology, Patiala during January, 2018 to July, 2018. No part of the matter embodied in this report has been submitted to any other university or institute for the award of any degree.

Date: 30 / 06 /2018

Charu Goyal

It is certified that the above statement made by the student is correct to the best of my knowledge and belief.

Vijay Luxami

Dr. Vijay Luxami
Associate Professor
School of Chemistry and Biochemistry,
TIET, Patiala-147004

Dedicated to

My parents

ACKNOWLEDGEMENTS

After an intensive period of six months, today is the day writing this note of thanks is the finishing touch on my dissertation. It has been a period of intense learning for me, not only in the scientific area but also on a personal level. I would like to reflect on the people who have supported and helped me so much throughout this period.

I would first like to thank my advisor, Dr. Vijay Luxami, who expertly guided me through my research project. Her unwavering enthusiasm for chemistry kept me constantly engaged with my research, and providing me with an excellent atmosphere for doing research.

Secondly, I would never have been able to finish my dissertation without the guidance of my supervisors, help from friends, and support from my family. Hence, I would like to thank Mr. Gulshan Kumar for supervising my research for the past six months and helping me at each and every step in the entire process of my dissertation. I would also thank other research scholars Ms. Richa Bansal, Mrs. Ruhi Mehta, Mr. Iqbal Singh, Ms. Sudesh Rani, Ms. Aastha Palta, for helping me and guiding me in their best possible way. I would also thank my classmates Manveer, Akanksha, Jasleen for providing me constant support throughout the project. I am further grateful to Dr. Amjad Ali (Head of Dept.) and all the faculty members for their assistance. I would also like to acknowledge SAI Labs and Punjab University, Chandigarh for providing the NMR and Mass Spectrometry facilities respectively.

In the end, I want to thank my family especially my parents for being pillars of strength and always being so supportive of me and encouraging me with their love and best wishes.

Charu Goyal

Abstract

Two chemosensors (6-amino-5-(((2-hydroxynaphthalen-1-yl)methylene)amino)-2-mercapto pyrimidin-4 **(Probe 1)** and 3,3'-bis(benzo[d]thiazol-2-yl)-[1,1'-binaphthalene]-2,2'-diol **(Probe 3)** were synthesized for Al^{3+} detection and OCl^{-} detection via fluorometric approaches. Probe 1 displayed shift in absorption spectrum in presence of Cu^{2+} metal ions from 420 nm to 450 nm. And enhancement in fluorescent spectrophotometer from in presence of Al^{3+} metal ions from 420 to

520 nm. On the other hand, Probe 3 do not show any change in absorption spectrum on addition of any metal ion. But show enhancement in emission spectrum at 420 nm. Therefore, Probe 1 shows fluorogenic response towards Al^{3+} metal ion in aqueous methanol medium and Probe 5 shows fluorogenic response towards OCl^{-} ion in aqueous ACN medium. Probe 1 contains benzothiazole unit and probe 3 contains BINOL unit.

LIST OF ABBREVATIONS

NMR	Nuclear magnetic resonance
TLC	Thin Layer Chromatography
PET	Photo induced Electron Transfer
ICT	Intramolecular Charge Transfer
CN^-	Cyanide ions
SCN^-	Thiocyanate
OAc^-	Acetate anion
HSO_4^-	Sulfate anion
$H_2PO_4^-$	Dihydrogen Phosphate Anion
NO_3^-	Nitrate anion
F^-	Fluoride ions
Br^-	Bromide ions
Cl^-	Chloride ions
OCl^-	Hypochlorite ion
Na^+	Sodium cation
Mg^{2+}	Magnesium cation
K^+	Potassium cation
Al^{3+}	Alminium cation
Cr^{3+}	Chromium cation
Fe^{3+}	Ferric cation
Co^{2+}	Cobalt (II) cation
Ni^{2+}	Nickel cation

Cu^{2+}	Cupric cation
Zn^{2+}	Zinc cation
Pd^{2+}	Palladium cation
Hg^{2+}	Mercuric cation
Ag^{+}	Silver cations
DFT	Dry Film Thickness
FTIR	Fourier-transform infrared spectroscopy
IR	Infrared spectroscopy
HOMO	Highest Occupied Molecular Orbital
LUMO	Lowest Unoccupied Molecular Orbital
DMSO	Dimethyl sulfoxide

TABLE OF CONTENTS

Chapter 1 INTRODUCTION

Supramolecular chemistry is basically designing of new molecular design with the excellence of specific and sensitive reorganization of various different analytes. These molecular designs contain recognition and signaling moieties as necessary components employed with completely different ways and mechanisms like photo induced electron transfer, intramolecular charge transfer, etc.[1]

The molecular architect referred to as the chemosensors that manufacture the optical signals on binding to analytes (cations, anions etc.) via non-covalent interactions. Chromophore and fluorophore are the signaling units that imparts color changes and shows variation in the spectrum upon excitation. The recognition unit contains hetero atom which is capable of binding to analytes. The recognition unit is often abiotic in nature, benefits of high affinity, high specificity, and sensitivity. The analyte attached to binding unit alter the electronic surroundings of molecular structure as a consequence further changes the absorption and emission signals.[2] Analytes reaction will be reversible and irreversible in nature. In presence of matter and energy chemosensors convert chemical info into analytical signals. Supramolecular chemistry deals with the molecule with weaker interactions whereas ancient chemistry supported the valence bonding. Supramolecular chemistry includes molecular self-assembly, folding and recognition of molecules.[3] The neutral and ionic species wide found in physiology, catalysis and environmental chemistry. Because of the ever increasing concentrations of industrial chemical and agriculture pesticides, the presence of cations and anions within the surroundings, chemosensors are therefore starting to realize several applications. The simple example of supramolecular chemistry is fluorescent chemosensors which are based on chemical reactions for anions. The detection of reactive anions (reactive oxygen (ROS) and nitrogen (RNS) species) are done by fluorescent chemosensors. By the one-electron reduction of molecular oxygen, the

O^{2-} ion is generated.[4] Thus, the relation between O_2^- fluxes is of great importance. This interactions result in formation of supramolecular compounds. Fluorescent chemosensors are amongst the most common kinds of optical sensors as a result of they are straightforward, cheap, sensitive and simple to use. Fluorescent chemosensors based-on differing types are extensively accustomed find the various categories of analytes together with organic analytes, metal cations, anions,

explosives, thiols, and gases. Within the design of a fluorescent chemosensor, there are 2 main units, the recognition (receptor) and signal moieties (fluorophore). Generally, they are covalently connected to every alternative.[5] The target analyte by selection binds to the receptor and also the fluorophore converts this binding event into a fluorescence signal. The binding of analyte will occur via a covalent bond *via* a non-covalent reversible

interaction. The non-covalent interactions between receptor and analyte embrace H bonding, electrostatic interactions, metal chelation, π-π or cation-π interactions, or reversible bond formation together with element acid-boronate and imine bonds.[3] The kind of the modification within the fluorophore signal upon binding process are often expected. These changes may be quenching or enhancement of the fluorescence signal, similarly as red or blue shift within the emission wavelength of the fluorophore. There are generally two types of design in fluorescent chemosensors which are the:

Fluorophore-spacer-receptor type
The integrated fluorescent type probes

In the fluorophore-spacer-receptor chemosensors there is a spacer between the receptor and the fluorophore which interrupts the electronic communication between receptor and signaling unit. As a result, photo-induced electron transfer (PET) occurs between the units. Thus, there is either amplification or quenching of the fluorescence signal upon binding of analyte to the receptor. In the mechanism of PET, there are two different energy levels belonging to the fluorophore and receptor units in the system.[6] Upon excitation of the fluorophore, one electron is promoted from the HOMO to the LUMO. This enables electron transfer from HOMO of the receptor to that of the fluorophore resulting in fluorescence quenching.[7] However, upon binding of an analyte to the receptor, the bound-receptor HOMO becomes lower in energy and electron transfer is inhibited, resulting in the restoration of fluorescent emission.

BINOL is an organic compound that is often used as a ligand for transition-metal catalyzed asymmetric synthesis. BINOL are used to synthesize chiral fluorescent sensors, which are used to carry out high enantioselective and sensitive recognition of chiral amino alcohols and amino acid derivatives.[8] By inducing suitable functional group in BINOL, the chiral property can be enhance. BINOL has a great importance for its chirality in extensive applications in molecular recognition, asymmetric synthesis and materials. For detection of anions, cations, and amino acids, a large number of fluorescent chemosensor based on BINOLs were synthesized.[9]

Chapter 2 LITERATURE STUDIES

Aluminum is one of the crucial element in earth's crust. Free aluminium is obtained in surface water and in environment due to effect of acid rain. From last few years, aluminium is used drastically in our daily activities such as cooking utensils and aluminum foil. Due to increase in amount of aluminum metal ion, it starts causing adverse effect on the environment. Aluminium is used in daily food, aeronautic transport, space industries, construction, packaging and aluminum- based pharmaceuticals.[10] Aluminium is toxic in nature and its toxicity causes a large number of diseases such as, Parkinson's diseases, Alzheimer's disease, etc. According to World Health Organization, 7.0 mg/Kg tolerable limit of aluminium ion by a human body in a week, this amount is found on the basis of short term toxicity. To prevent the harmful effects on the human beings and environment by Al^{3+}, the concentration of Al^{3+} in the nature is needed to be controlled to prevent the adverse effects on biosphere and on human being. The detection of the aluminum ion concentration is not easy, due to insufficient spectroscopic characteristics.[11] Therefore, it is required to generate more Al^{3+} sensors, which possess easy synthetic route, selective mechanisms and are sensitive in nature.

Hypochlorite (OCl^-) is widely used in disinfection of drinking water, and cyanide treatment. OCl^- are very reactive in nature, so they are used within in the range of $10–10^{-4}$ μM concentration. OCl^- plays an important role in the immune system of the living organisms.[12] But owing to its high reactivity and no specificity, excessive production of OCl^- can lead to damage of host tissue and which lead to severe human diseases.[13] Long-term exposure to the high concentration of chlorine in water, leads to eyes irritation and cause stomach problems. Thus, OCl^- detection is required.

2.1 Literature Review:

Lu *et al.* synthesised a unique imidazolium-functionalized BINOL fluorescent probe **1** and analyzed its chiral and chromogenic recognition properties toward various forms of anions.[14] In distinction to most fluorescent sensors for F^-, probe **1** showed wonderful property for F^- over interfering anions such as $CH_3CO_2^-$, CN^- etc. This specialty may even be attributed to the distinctive speedy charge-transfer emission response evoked by F^-. In the presence of

various anions R-1 was excited at 365 nm. The fluorescence spectra show a distinct and very intense peak at 454 nm with CH_3CO^{2-} and 474 nm with F^-.

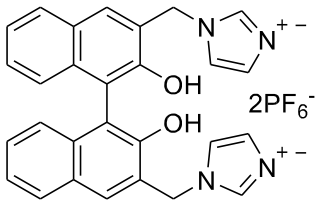

1

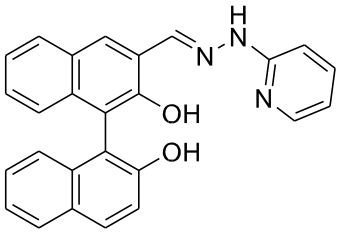

2

Jiao *et al.* reported a fluorescent sensors supported BINOL for Zn^{2+}. Probe **2** was extremely selective and ratiometric for Zn^{2+}. Especially, probe **2** wasn't full of Cd^{2+}.[15] Confocal microscopy experiments prompt that probe **2** might be successfully penetrate in live cells. In addition, the ISRE (Importance of two inferno stimulated response element) showed higher property to Histidine within the presence of various amino acids and perceived Histidine through a displacement mechanism. Probe **2** displayed weak fluorescence emission at 500 nm, upon gradual addition of

Zn^{2+} to the probe, the emission intensity at around 500–550 nm increased significantly.

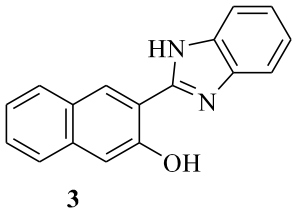

3

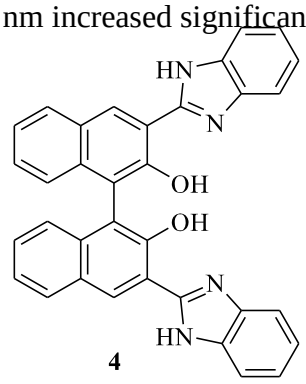

4

Luxami *et al.* developed a fluorescent probe **3** and **4** for the selective estimation of Zn^{2+} and Cu^{2+} metal ions and a ratiometric sensing of Zn^{2+} metal ions.[16] Probes **3** and **4 (**CH_3CN–H_2O; 4: 1) at pH scale 7.0 $\pm$ 0.1 (10 µM, HEPES) showed selective binding with Zn^{2+} ions and provides a replacement emission band at 490 nm. Probe **3** estimate 20 nM Zn^{2+} ions because of the low detection limit. The determination of Zn^{2+} ions by probe **3** wasn't interfered by presence of different metal ions viz. K^+, Na^+, Mg^{2+} ,Ca^{2+}, Fe^{2+}, Sr^{2+}, Ni^{2+}, Ag^+, Co^{2+}, Cd^{2+}, Hg^{2+}. However, within the case of probe **4**, in ACN, the addition of various concentrations of Cu^{2+} (2 µM, 5 µM,

10 µM) and a hard and fast quantity of F2 (25 µM) to an answer of 2 (0.25 µM, CH_3CN) elaborates

Cu^{2+} metal ion concentration dependent NOR, antibacterial and Boolean operators with distinct

emission channels at 585, 515 and 400 nm, severally. Fluorophore probe, although amphiphilic in nature, doesn't permit elaboration of logic gates. The effect of varied structural options on Probe- in elaborating logic operations is being investigated.

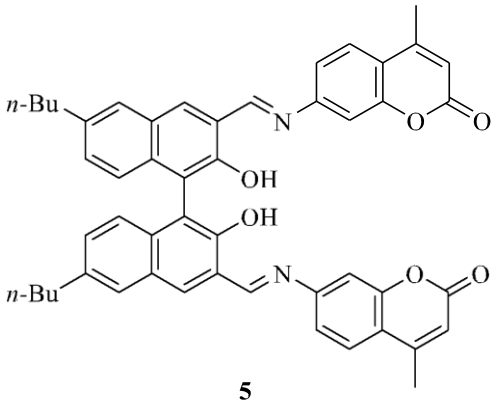

5

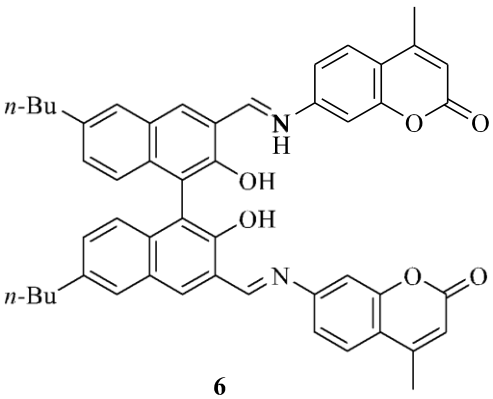

6

Jiao *et al.*, report a chiral probe **5** contains (S)-BINOL substituted moieties. These moieties were synthesized via a Nu^- addition and elimination reaction.[17] Reduction reaction of the imine-based probe **5** with $NaBH_4$, probe **6** was synthesized. With the help of Ultra-Violet spectrum the fluorescence responses of the chiral compounds (Probe **5** and Probe **6**) on Laevo and Dextro rotatory phenylalaninol were investigated. The intensity of light of Probe **5** in cooperation with Laevo and Dextro rotatory phenylalaninol shows a gradual improvement and it keeps a virtually linear correlation with molar concentration ratios from 1:10 to 1:180. A calculations were done to determine Stoichiometry's and the association constant of probe **5** with Laevo and Dextro rotatory phenylalaninol and results showed that the chiral detector probe **5** will exhibit an intersesting

''turn-on'' emission and wonderful enantioselective behaviour for the Laevo rotatory phenylalaninol. On the other hand, no fluorescence effect detected for probe **6** towards Laevo and Dextro rotatory phenylalaninol. Phenylalaninol was excited by a commercially available UV lamp (λ = 365 nm). When probe **5** was treated with an excess amount of Laevo or Dextro rotatory phenylalaninol, the fluorescence intensities centered at (λem = 409 nm) show a gradual enhancement.

Liu *et al.* synthesized and have incorporated amino alcohol units to the foremost necessary groove of BINOL to construct new chiral fluorescent sensors **7** and **8**.[18] Fluorescent study

of these compounds has clarified a previous misconception. The usually accepted acid inhibition of the PET fluorescence ending inside the aryl-amine sensors is not involved inside the fluorescent

responses of the BINOL-amine primarily based sensors at all. This can be often to keep with the physical science argument on the concept of the reaction potentials of the alkane series donors and additionally the phenol acceptors. The greatly redoubled fluorescence of probe **7** and probe **8** inside the presence of the chirality-matched mandelic acid got to result to the formation of the structurally more rigid fluorophores upon acid complexation, the suppressed excited state heavy particle transfer and additionally the isolation of the fluorophores inside the solid state. This work has provided a stronger understanding for the mechanism of the fluorescence response of the BINOL- based sensors. Probe-**7** shows dual emission at λ = 439 nm, but the major-groove isomer Probe **8**

gave only the short wavelength emission at λ = 379 nm.

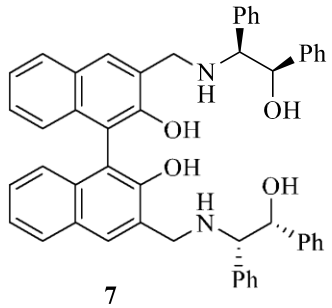

7

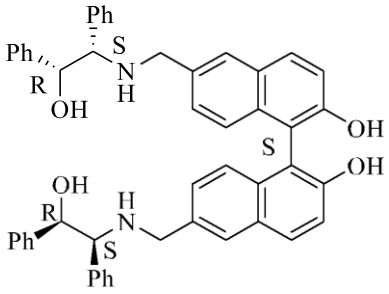

8

Yang *et al.* synthesized imidazolium chemosensor which are binapthyl based system, for highly selective recognition of essential amino acid like Tryptophan among the 11 amino acids in liquid solutions via multiple gas bonding and also synergistic effects of static interactions.[19] Probe **9** is a structurally open receptor which exhibits plenty of significant property. Receptors probe **11** and **12** shows low affinity towards L-Tryptophan than probe **9**. The macrocyclic probe **11** exhibits a remarkable chiral recognition capability for the 2 enantiomers of tryptophan, despite associate low selectivity towards a range of aromatic amino acids, through methylation of the C-2H of the imidazolium nucleus of probe-**10**. The imidazolium ring was analysed as a strong hydrogen-bond donor. Fluorescence spectra of in aqueous solutions at λ_{exc} = 336 nm, 327 nm and 327 nm, respectively.

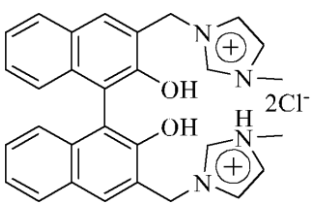

9

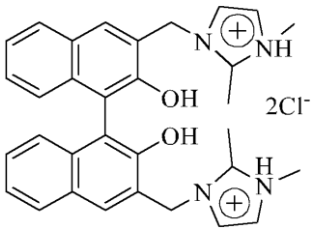

10

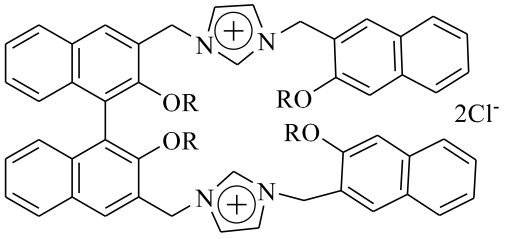

11 and 12

R = CH_3OCH_3 **(11)**

R = CH_3 **(12)**

Gupta *et al.* synthesized and designed naphthoic acid based hybrid molecular and investigated their photophysical behavior towards different metal ions and anions.[20] The probe **13** has been used for the selective estimation of Al^{3+} metal ions. The binding event signaled through formation of new absorption band at 405 nm and 'turn-on' fluorescence band at 505 nm. The probe **13** showed selective estimation of CN^- and OH^- ions among all other anions by forming new absorption band
at 400 nm and fluorescence 'turn-on' at 520 nm.

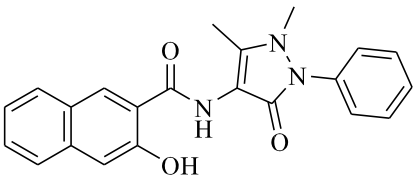

13

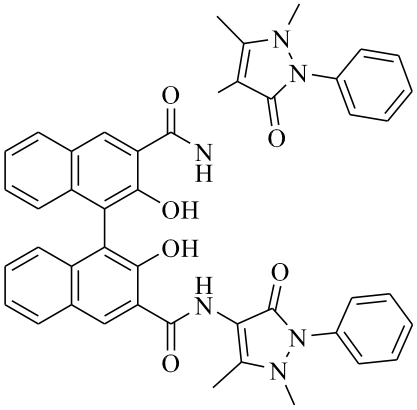

14

Gupta *et al.* developed a BINOL based probe **14** having diamide cluster and investigated the photo physical behavior towards various ions.[21] The probe **14** has been used for detection of Al^{3+} and Cu^{2+} metal ion as compared to different metal ions and signaled the binding event through formation of absorption bands at 415 and 430 nm. Differential emission bands area unit shaped within the presence of Al^{3+} at 515 nm and Zn^{2+} at 485 nm whereas conclusion is discovered just in case of Cu^{2+} ions. The probe **14** shows selective estimation for CN^- ions among all different anions by forming new optical phenomenon at 395 nm and emission band at 495 nm.

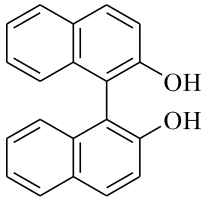

15

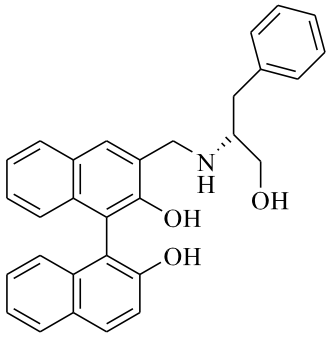

16

Dong *et al.* synthesized a chemosensor bearing (R)-OH associate amino chemical group (probe-**15**), for the extremely selective fluorescent recognition of the Al^{3+}.[22] *"Turn-on"* kind visible radiation changes were discovered upon the addition of Al^{3+} in solution. The numerous enhancement (35.4-fold) of visible radiation intensity was ascribed to the complicated formation between (R)-OH and Al^{3+} that denoted because the chelation-enhanced fluorescence method. Fluorescence property of BINOL-b-amino alcohol conjugate (R)-OH has been studied. It still shows Al^{3+} selective fluorescence enhancement that originates from CHEF (chelation-enhanced fluorescence) by coordination association with Al^{3+} ions. The comparison of its sensing skills with previous receptor probe **16** discovered that terminal –OH or –COOH cluster is that the key binding website for the high property for Al^{3+} over different metal ions. free (R)-OH exhibits single fluorescence emission band at 370 nm, upon the addition of Al^{3+}, a fluorescence enhancement was observed from 370 to 375 nm.

Velumugran *et al.* designed and synthesized a straightforward dimeric binol-based fluorescent chemosensor probe **17** that exhibited an extremely selective detection of Hg^{2+} in liquid media and in presence of all different metal ions at neutral hydrogen ion concentration.[1] The Hg^{2+} recognition processes follow a photograph elicited lepton transfer mechanism and are scarcely influenced by different synchronic metal ions. Additionally, determination of mercury in waste water samples was additionally analyzed. The sizeable sweetening with high emission property of probe **19** toward Hg^{2+} is because of excite electron transfer inhibition method within the complicated molecule. Moreover, the detection limit of receptor probe **17** toward Hg^{2+} was 4×10^{-7} M that indicated that the sensing element probe **17** are often helpful

for biological, pharmacology and environmental applications. Probe **17** shows the absorption band at 335 nm in the UV–vis

spectrum, in the presence of various concentrations of Hg^{2+}, it shows fluorescence spectrum at 375

nm.

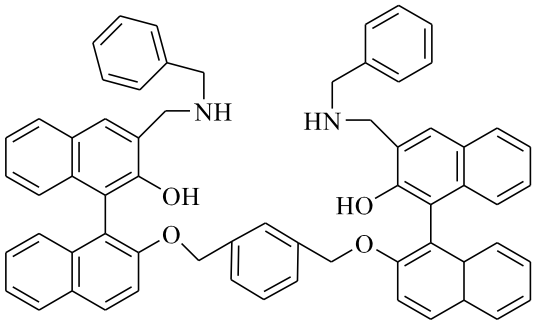

17

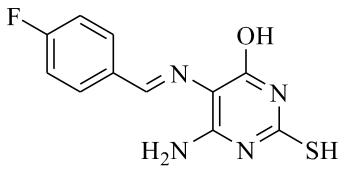

18

Maurya *et al*. designed and synthesized a novel simple pyrimidine based Schiff base probe **18** that showed colorimetrical and fluorescence "turn on" sensing behavior towards Ag^+ in Dimethyl formamide (50%).[23] The probe **18** express quick, selective and sensitive signal towards Ag^+ with low detection limit of 1.12×10^{-6} M with no interference. The studies discovered the binding mode between probe **18** and Ag^+ 1:2 that additionally supported by nuclear magnetic resonance titrations, EDX technique and Density Functional Theory calculations. Electrochemical study was used to explore the interaction between probe, Ag^+ and CN^-. Contemporary the subsequent silver complex ensemble with CN^- unconcealed fluorescence quenching because of formation of $[Ag(CN)x]^-$ species via displacement approach. The probe was much applied for strip check kit that served as mini colorimetrical device for detection and analysis of Ag^+ and CN^- in pure water samples and results were compared with Atomic Absorption Spectroscopy. Probe 18 showed two absorption band at 290 and 362 nm due to π-π*, n-π* transition and gave colorless solution. After addition of Ag^+ fluorescence intensity enhanced at 425nm.

Gupta *et al.* synthesized novel efficient pyrimidine based receptors **19** and **20** via facile condensation method and were characterized by numerous techniques. After different metal ions addition, each receptor display an interesting modification in color. By use of Ni (II) metal ions receptor showed change in color from yellow to dark yellow, that makes it appropriate for simple eye detection. The Job's plot, Electron Spray Ionization Mass Spectroscopy and ^1H

nuclear magnetic resonance titrations confirmed stoichiometry of probe **19** and **20** and Ni (II) as 2:1. A lot of interestingly, fluorescence titration disclosed that probe **19** and probe **20** behave nearly as superb

fluorescence quenchers. The LOD has been calculated to be 33 for Probe **19** +Ni (II) and 48Mm for probe **20** +Ni (II), which indicates probe **20** is inferior to probe **19**. By cyclic voltammetry experiment, electroanalytical studies were investigated. Upon addition of nickel metal ions, probe **19** and probe **20** achieved electrochemical changes and chemical reaction potential. Density Functional Theory calculations have unconcealed that upon coordination with the Ni(II) , the energy gap between the LUMO and HOMO of probe **19** and **20** has considerably reduced within gas phase.[24] Probe **19** showed the maximum excitation at 392 nm and emission at 520 nm while Probe **20** showed the maximum excitation at 374 nm and emission at 441 nm which shows a large
stoke shift.

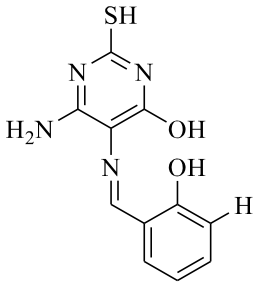

19

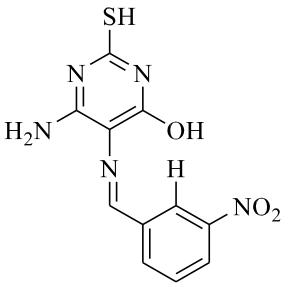

20

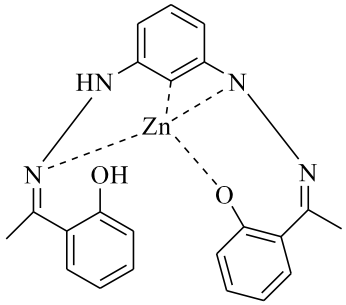

21

Mati *et al.* reported extremely selective fluorescent detection of Zn ions. A Schiff-base complex was synthesized and designed i.e PyMD (Probe **21**).[25] In 1:4 water-methyl alcohol mixture, Zn ions binding promote the ~23 fold fluorescence enhancement of probe **21** at wavelength of 469 nm. The LOD of Zn^{2+} ions was calculated to be 6.9×10^{-7} M consistent with fluorometric titrations. By combined UV–visible, nuclear magnetic resonance, fluorescence, and HRMS spectroscopically strategies, established the 1:1 binding mode of the metal complexes. Photo physical investigations together with time resolved analysis and steady-state recommended a mechanism for the fluorescent Zn ions, involved a ligand-to-metal charge transfer pathway. The experimental observations of the free sensor molecule (PyMD: probe **21**) and also the complexed structures of (PyMD-Zn^{2+}) were confirmed by DFT calculations. Finally, for detection of the free Zn ions in samples, a newly synthesized PyMD was applied, e.g., banana juice, cabbage, and beverages. Besides, for

cell imaging study of E.coli, fluorescence behavior of complex PyMD-Zn^{2+} was extensively utilized. The absorption spectrum of PyMD has two λabs max, centered at 290 nm and 335 nm, respectively. The first band at 290 nm attributed to

the second band at 335 nm. With varying solvent polarity from MeOH to n-Heptane λ_{abs}^{max} = 290 nm was observed to be shifted at 285 nm. With gradual increase of Zn^{2+} concentration, intensity at 290 nm was increased and the band at 335 nm was gradually decreased and a new band formed at 375 nm.

Maurya *et al.* has synthesized a novel molecular receptor **22**–Co^{2+} complex that exhibited an amendment in optical properties with CN^- (0.12 μM) via a complexation methodology. Moreover, CN^- binding powerfully perturbs oxidation and reduction properties of the probe **22**–Co^{2+} complex. The attainable binding mode was confirmed by studies of nuclear magnetic resonance, Infra-red spectroscopy and mass spectrometry. The sensible relevance of probe **22** as an implication to logic gate supported the emission changes with the input of CN^- and Co^{2+} was investigated.[26] The system was applied as a logic gate supported, due to emission band at 431 nm. Probe **22** exhibited a characteristic absorption band at 344 nm, upon gradual addition of Co^{2+}, the band at 344 nm shifted towards the blue region at 332 nm with a clear convergence
point at 303 nm.

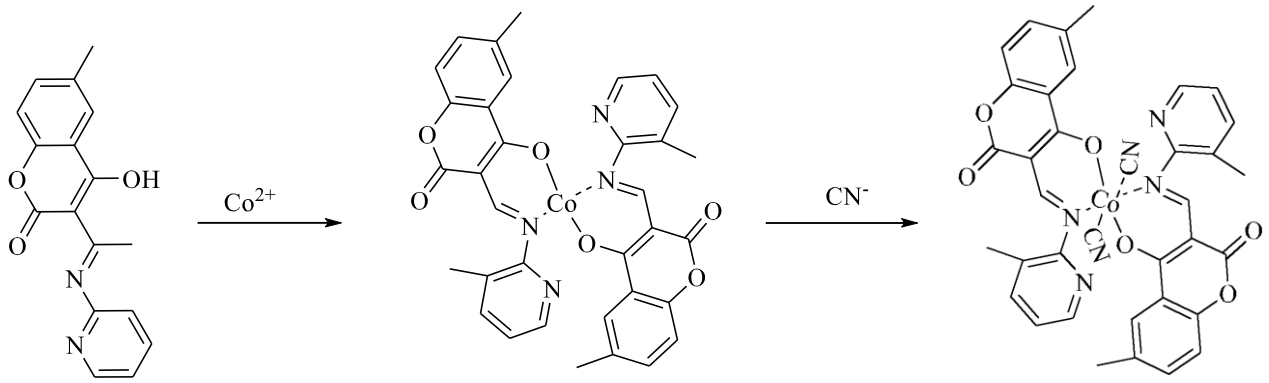

22

Min *et al.* synthesized and developed sensitive and selective colorimetrical detector probe **23** that was capable of detection of Cu^{2+}, Co^{2+} and S^{2-} via the optical method in liquid media. It may by preferentially monitor and select Cu^{2+} and Co^{2+} over different competitive ions. Additionally, probe **23** showed terribly low detection limits for Cu^{2+} (0.19 μM) and Co^{2+} (0.18

μM), that were a lot of below the rules for Cu^{2+} (31.5 μM) by the World Health Organization and Co^{2+} (17 μM) by

the independent agency. Significantly, probe **23** was used to practical chemosensor to find the quantity of Cu^{2+} and Co^{2+} in real water samples.[27] Moreover, probe **23** additionally displayed extremely selective and discriminatory recognition toward S^{2-} by a color modification. Apparently, probe **23** was the initial example of a chemosensor which can estimate 3 analytes ie. Co^{2+}, S^{2-}, and Co^{2+}, effectively and simultaneously. Moreover, the sensing mechanisms of probe **25** for Cu^{2+}, Co^{2+} and S^{2-} were explained by the theoretical calculations. Probe **23** exhibited a maximum absorption at 375nm. Upon gradual addition of Cu^{2+} to probe **23**, the absorption bands at 280 nm and 450 nm increased and the band at 375 nm decreased gradually

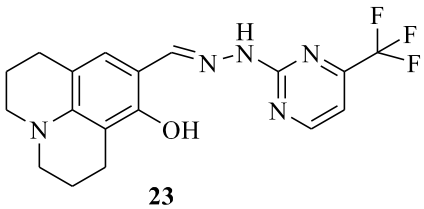

23

2.2 RESEARCH GAP IN STUDY:

Heterocyclic molecular architectures have been widely used for tunable photo physical properties and have been successfully utilized as chemosensors. The mercaptopyrimidine based molecular system have wide application in biological systems, yet it was least explored for its photophysical and sensing properties. Also, the benzothiazole based system have been known for their photophysical and sensing properties. On the other hand, there is another class of molecules known as BINOL, which have used in logic gate preparation, sensors for various metal ions, anions and biological important species. However, there is no report where benzothiazole units have been incorporated on BINOL molecular systems. To address the question of photo physical behavior of benzothiazole based BINOL, and Schiff based containing pyrimidine units, have been designed as objective for the present study.

2.3 OBJECTIVE

Our aim was mainly concerned with synthesis of BINOL based molecule and its applications as a fluorescent sensor for common metal ions and anions. Thus, the main objectives of the present thesis are:

Incorporation of heterocyclic benzothiazole architect on BINOL platform.

To investigate the photophysical behavior of synthesized BINOL-benzthiazole molecular assemble.

To synthesize and evaluate the photophysical properties of Schiff base of pyrimidine and naphthol system.

Chapter 3 EXPERIMENTAL SECTION

3.1 Materials, Methods and Instrumentations:

All the chemicals which are used in synthesis of compounds were purchased from Sigma-Aldrich Chemical Limited, Loba Chemie relying upon their availability. The solvents used were of spectroscopical grade purchased from the Spectrochem Limited. All chemicals and the solvents were of high purity. By the means of thin-layer chromatography, the reaction progress was monitored. The melting points were recorded by the open capillary tube technique. ^{1}H NMR and ^{13}C NMR spectra were recorded on instrument JEOL ECS-400 MHz spectrometer at ambient temperature. In $CDCl_3$ or/and DMSO (d_6) NMR samples were prepared and TMS used as an internal reference. All the chemical shifts were reported in parts per million relative to the reference. The stock solutions of varied cations of concentration 1×10^{-1} $molL^{-1}$ were ready to create their corresponding salts. Tetra butyl ammonium ion salts were taken as anions. A stock solution of ligands was prepared at 10^{-3} M (25mL). For photo physical studies in various solvents diluted solvent is used. The absorption spectra were recorded on SHIMADZU-2600 spectrophotometer. The quartz cuvettes of 1 cm in path length were used in spectrophotometer. The fluorescence spectra was recorded on a Varian Carey Eclipse fluorescence spectrophotometer using a slit width excitation = 20 nm and emission = 20 nm at stated excitation. By Jobs Plot the stoichiometry of complexes was determined. The Benesi-Hildebrand equation was used for determining stability constant.

UV-vis And Fluorescence titrations:

The stock solutions of various metal ions and anions of the concentration 1×10^{-1} $molL^{-1}$ were prepared from their corresponding salts. Tetra butyl ammonium ion salts of various anions such as CN^-, SCN^-, OAc^-, HSO_4^-, $H_2PO_4^-$, NO_3^-, F^-, Br^-, Cl^-, OCl^- were taken. Perchlorate salts of various metal ions such as Na^+, Mg^{2+} , K^+, Al^{3+}, Cr^{3+}, Fe^{3+}, Co^{2+}, Ni^{2+}, Cu^{2+}, Zn^{2+}, Pd^{2+}, Hg^{2+}, Ag^+, etc. were used. A stock solution of probe **1** and probe **3** was prepared in CH_3CN

and DMSO respectively at 10^{-3} M (25mL). All the UV-Vis and fluorescence studies of probe 1 were done in CH_3OH: H_2O (9:1) and that of probe 3 in CH_3CN: H_2O (9:1).

3.2 Calculation of binding constant and limit of detection:

The binding constants of ligands for various analyte were determined by following the Benesi-Hildebrand equation:

$$\frac{1}{I - I_0} = \frac{1}{K_a(I_{max} - I_0)[C]^n} + \frac{1}{I_{max} - I_0}$$

Where I_0, the absorption/emission intensity of the ligand in absence of analyte, I is the absorption/emission intensity of the ligand at an intermediate analyte concentration, and I_{max} is the absorption/emission intensity of the ligand at a concentration of complete interaction with analyte respectively. K_a is the binding constant, C is the concentration of analyte and number of analytes bound per ligand molecule is represented by n. The detection limit (DL) is determined from the following equation:

$$DL = \frac{K \times Standard\ deviation\ of\ the\ blank\ solution}{slope\ of\ calibration\ curve}$$

Where K = 2 or 3

3.3 Job's Plot

Various number of solutions containing ligand and TBACN were prepared such that the sum of the total anion and ligand concentration remained constant. The mole fraction (X) was varied from

0.1 to 1.0. The intensity at respective wavelength was plotted against the molar fraction of the Cu^{2+}

Solution.

3.4 Synthetic Experimental Table:

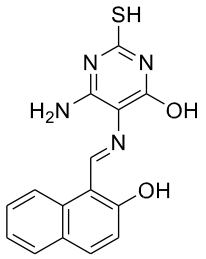

1

Yield. 80%; M.pt. 150 ºC, ^{1}H NMR (DMSO-d_6, 400MHz, δ/ppm) 14.22 (s, 1H, OH), 10.50 (s, 1H, SH), 8.10 (d, *J* = 8.4, 1H, ArH), 7.87 (m, *J* = 7.6, 2H, ArH), 7.54 (t, *J* = 6.8, 1H, ArH), 7.35 (t, *J* = 4.8, 1H, ArH), 7.12 (d, *J* = 8.4, 1H, ArH), 6.54 (s, 1H, ArH), 5.66 (s, 1H, ArH).

^{13}C NMR (DMSO-d_6, 100MHz, δ/ppm) 171.85, 167.9, 160.2, 157.6, 155.1, 150.4, 133.5, 132.4, 128.9, 127.6, 123.2, 120.02, 119.3, 110.5, 101.9.

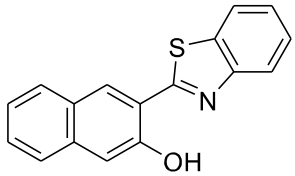

2

Yield = 70%; m.pt. 180ºC; ^{1}H NMR (400 MHz, $CDCl_3$) δ(ppm): 12.27, (s, 1H, OH) (8.26 (s, 1H, ArH), 8.04 (d, *J* = 8.4 Hz, 1H, ArH), 7.95 (d, *J* = 7.6, 1H, ArH), 7.84 (d, *J* = 8.4, 1H, ArH), 7.72 (d, *J* = 8.4, 1H, ArH), 7.53 (m, 4H, ArH), 7.35 (t, *J* = 6.8, 1H, ArH), 7.26 (s, 1H, ArH); ^{13}C NMR (100 MHz, $CDCl_3$) δ(ppm): 169.08, 154.2, 151.9,
136.1, 132.8, 129.2, 128.2, 128.1, 126.8, 126.3, 125.3, 123.9, 122.4, 121.5, 118.9, 111.8.

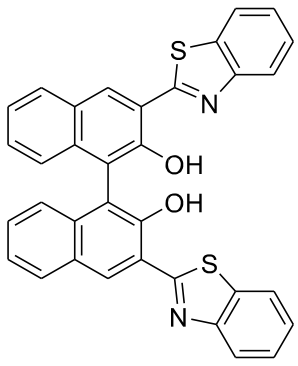

3

Yield = 56%; M.pt. 200ºC, ^{1}H NMR (400 MHz, $CDCl_3$) δ (ppm): 9.00 (s, 1H, OH), 8.89 (s, 1H, OH), 8.20 (d, *J* = 8.4, 1H, ArH), 8.13 (d, *J* = 8.4, 1H, ArH), 8.06 (d, *J* = 8.4, 1H, ArH), 7.94 (m, 1H, ArH), 7.72 (t, *J* = 8.4, 1H, ArH), 7.54 (m, 2H, ArH), 7.42(m, *J* = 4, 4H, ArH), 7.26 (s, 1H, ArH); ^{13}C NMR (100 MHz, $CDCl_3$) δ (ppm): 162.7, 159.8,
155.02, 152.733, 151.9, 144.9, 143.3, 136.8, 136.05, 128.4, 126.2,
125.4, 124.9, 124.4, 122.9, 122.7, 122.4, 117.9, 116.2, 91.2.

4.1.1 Synthesis of (6-amino-5-(((2-hydroxynaphthalen-1-yl)methylene)amino)-2-mercapto pyrimidin-4 (1): Probe **1** was synthesized by adding 2-hydroxy-1-naphthaldehyde (1.5mmol,

0.2582g) in alcoholic solution of 5,6-diamino-2-mercaptopyrimidin-4-ol (1mmol, 0.1581g) with continuous stirring. 2 drops of glacial acetic acid was added to above solution as catalytic amount. The reaction mixture was refluxed for 12 hours. After completion of reaction (monitored by Thin Layered Chromatography), obtained dark yellow colored solid was filtered and wash with ethanol. A fine yellow color solid was obtained.

Yield. 80%.m.pt. 180ºC, ^{1}H NMR (DMSO-d_6, 400MHz) (**Figure 1**) δ (ppm) showed 1H singlet at δ 14.22 for OH (naphthalene), 1H singlet at δ 10.50 for SH, 1H singlet shown at δ 8.10 for ArH,

1H doublet shown at δ 8.10 for ArH, 2H multiplet shown at δ 7.87 for aromatic H, 2H multiplet shown at δ 7.54-7.35 for ArH, 1H doublet shown at δ 7.12 for ArH, 1H singlet shown at δ 6.54 for ArH, 1H singlet shown at δ 5.66 for NH bond; ^{13}C NMR (DMSO-d_6, 100MHz, δ/ppm) showed at

171.85, 167.9, 160.2, 157.6, 155.1, 150.4, 133.5, 132.4, 128.9, 127.6, 123.2, 120.02, 119.3, 110.5,

101.9 **(Figure 2)**. These ^{1}H NMR and ^{13}C NMR data corroborates with structure of probe **1.**

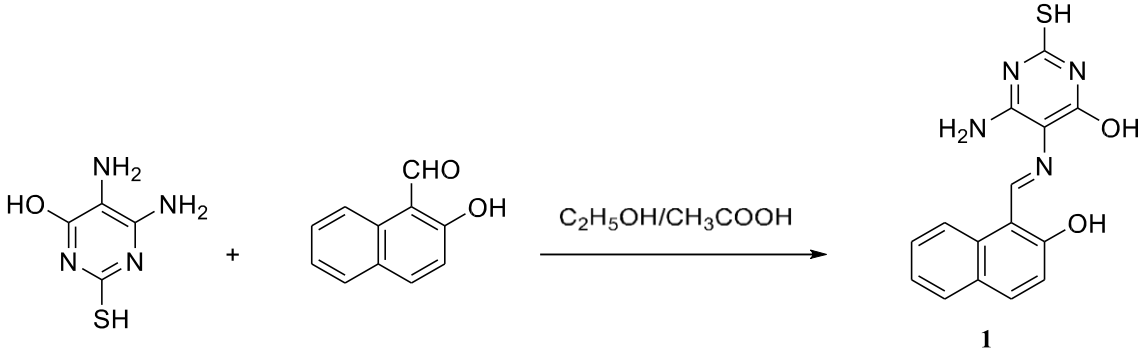

1

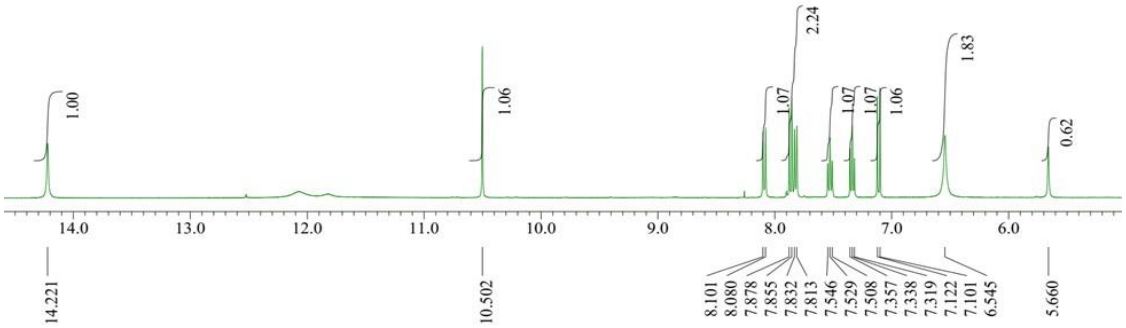

Figure 1. [1]H NMR of Probe **1**

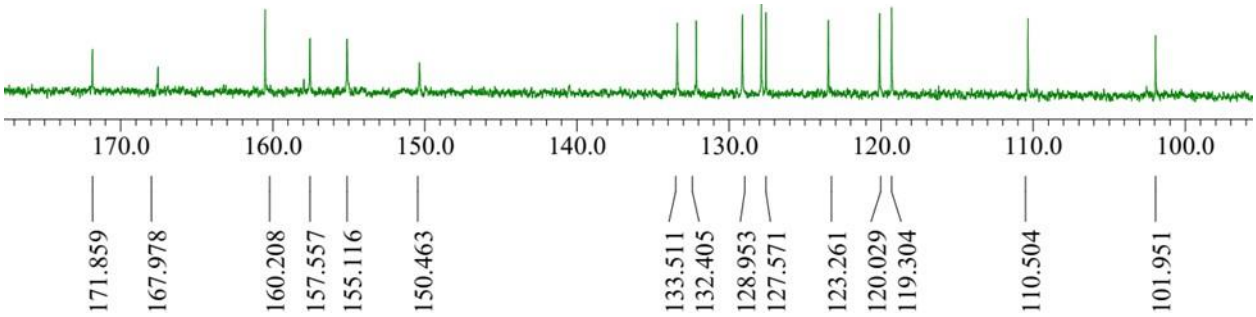

Figure 2. [13]C NMR of Probe **1**

4.1.2 Synthesis of 3-(benzo[d]thiazol-2-yl) naphthalen-2-ol (2): 3-hydroxy-2-napthoic acid (180 mg, 1 m moles) and 2-aminobenzenethiol (125 mg, m moles) were mixed in 3ml of Polyphosphoric acid. Further, the reaction was refluxed at 110 ºC for 8 hours. After the completion of reaction (monitored by TLC), the ice cold water was poured to the reaction mixture and yellow colored solid was obtained. The crude was filtered and washed with water. A fine yellow colored powder of compound **2** was obtained by column chromatography, hexane/chloroform (95:5; v/v) as the eluting solvent.

Yield = 70% m.pt. 180 ºC, ^{1}H NMR (400 MHz, $CDCl_3$) :1H singlet at δ 12.27 for OH, 1H singlet at δ 8.26 for ArH, 1H doublet δ at 7.95-7.72 for ArH, 4H multiplet is δ at 7.53 for ArH, 1H triplet at δ 7.35 for ArH, 1H singlet at δ 7.26 for ArH (**Figure 3**) ^{13}C NMR (100 MHz, $CDCl_3$) shown at δ (ppm): 169.08, 154.2, 151.9, 136.1, 132.8, 129.2, 128.2, 128.1, 126.8, 126.3, 125.3, 123.9, 122.4,
121.5, 118.9, 111.8. (**Figure 4**).

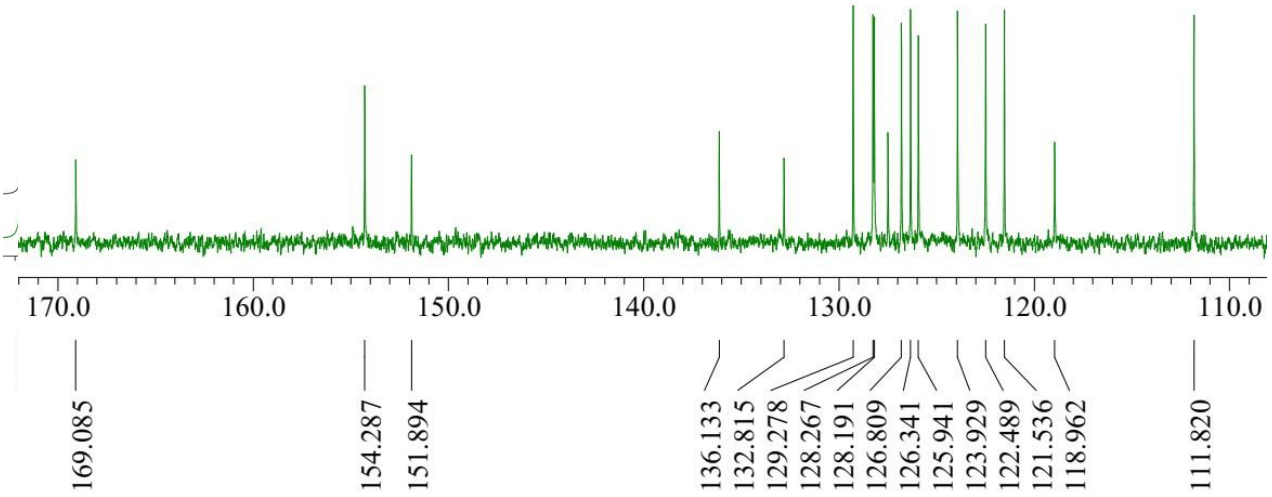

Figure 4. 13C NMR of Probe **2**

4.1.3 Synthesis of 3,3'-bis(benzo[d]thiazol-2-yl)-[1,1'-binaphthalene]-2,2'-diol (3): Compound

2 (350 mg) and catalyst Cu-TMEDA (5% mol %) were mixed in tetrahydrofuran (THF) and refluxed at 65 ºC. Yellow colored solid was obtained after 12 hours (reaction completion was monitored by thin layer chromatography). The reaction mixture was filtered and washed with the tetrahydrofuran. The impure product was purified by column chromatography using hexane/chloroform (50:50 v/v) as an eluting solvent. The purified compound was characterized through NMR technique.

Yield = 75% m.pt. 200ºC. ^{1}H NMR (400 MHz, $CDCl_3$): 1H doublet at δ 9.00 for OH (benzothiazole ring), 1H singlet at δ 8.89 for OH (benzothiazole ring), 1H doublet at δ 8.20-8.06 for aromatic H,
1H multiplet showed at δ 7.94-7.42 for ArH, 1H singlet at δ 7.26 for ArH (**Figure 5**); ^{13}C NMR

(100 MHz, $CDCl_3$) showed at δ (ppm): 162.7, 159.8, 155.02, 152.733, 151.9, 144.9, 143.3, 136.8, 136.05, 128.4, 126.2, 125.4, 124.9, 124.4, 122.9, 122.7, 122.4, 117.9, 116.2, 91.2 (**Figure 6**). These ^{1}H NMR and ^{13}C NMR corroborates with structure of probe **3.**

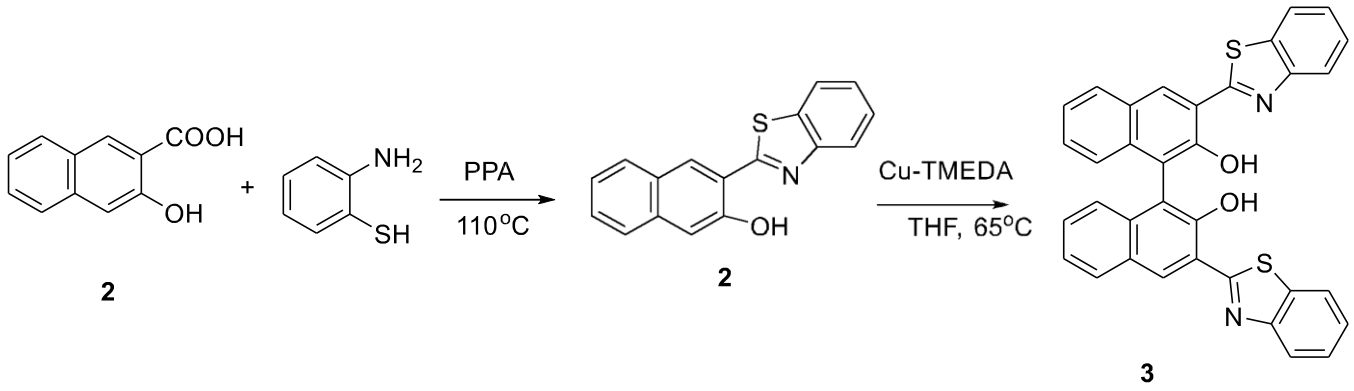

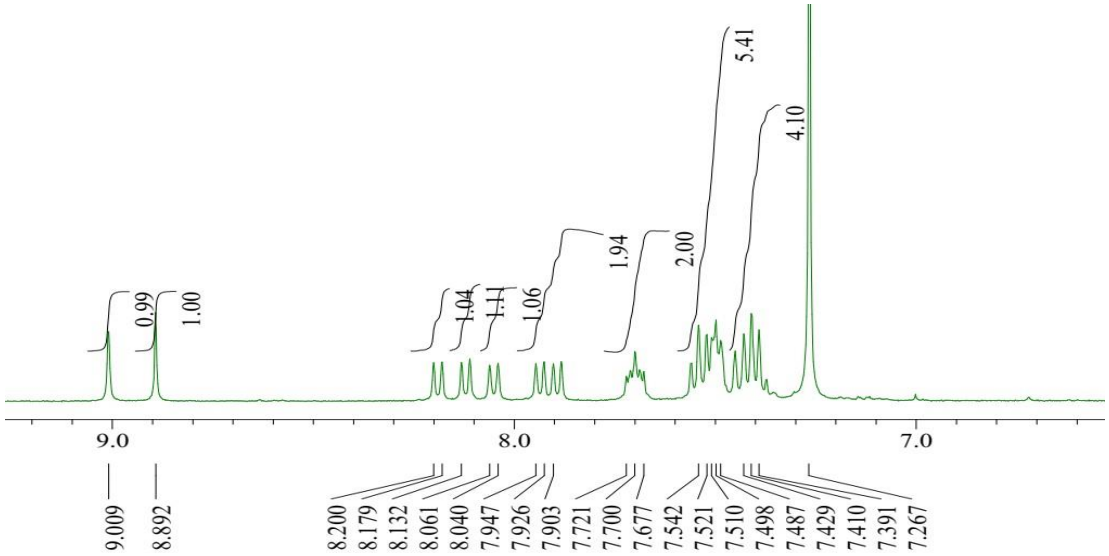

Figure 5: ^{1}H NMR of Probe **3**

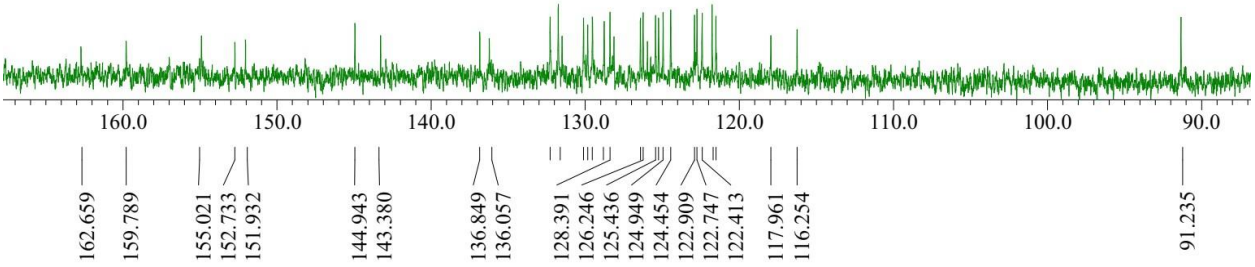

Figure 6. ^{13}C NMR of Probe **3**

4.2 Photo physical properties of Probe 1 and 3:

4.2.1 Absorption studies of Probe 1 towards metal ions:

The photo physical properties of probe **1** (10 µM in $CH_3OH:H_2O$: 9:1) were measured through absorption and emission spectroscopy. The absorption band of probe **1** showed maxima at 420 nm in CH_3OH/H_2O:9:1. Further, the recognition behavior of the probe **1** toward various cations, such as Na^+, Mg^{2+} , K^+, Al^{3+}, Cr^{3+}, Fe^{3+}, Co^{2+}, Ni^{2+}, Cu^{2+}, Zn^{2+}, Pd^{2+}, Hg^{2+}, Ag^+ was investigated by UV–visible and emission studies among different metal ions in CH_3OH/H_2O (9:1; v/v; HEPES pH

= 7.2) solvent system. On the introduction of Cu^{2+} ions to solution of probe **1** (10 µM in

$CH_3OH:H_2O$: 9:1) the absorption peak showed a red shift of 30 nm, however no other metal ions showed significant alteration in absorption peak (Figure **7**). Further, the gradual addition of Cu^{2+} ions, in the solution of probe **1**, resulted in new band at 450 nm, with small decrement in absorption

of probe absorption maxima.

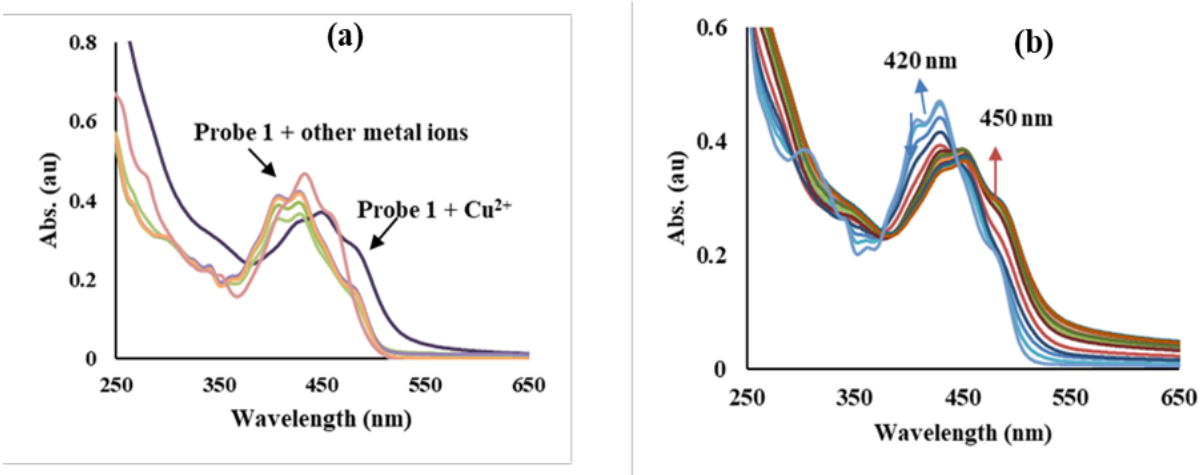

Figure 7. (a) UV–Visible spectra of probe 1 (10 µM in $CH_3OH:H_2O$::90:10) with absence and presence of different cations such as Na^+, Mg^{2+} , K^+, Al^{3+} , Cr^{3+}, Fe^{3+}, Co^{2+}, Ni^{2+}, Cu^{2+}, Zn^{2+} ,Pd^{2+}, Hg^{2+}, Ag^+ ions (b) Effect of increasing addition of $Cu^{2+}$to probe 1 (10 µM in CH_3OH/H_2O:9:1) on absorption spectrum.

4.2.2 Interferences studies of various metal ions:

To evaluate the relative interference of various cations in Cu^{2+} detection, the absorption responses of probe **1** to Cu^{2+} was measured in the presence of another cations i.e. Na^{+}, Mg^{2+} , K^{+}, Al^{3+}, Cr^{3+}, Fe^{3+}, Co^{2+}, Ni^{2+}, Cu^{2+}, Zn^{2+}, Pd^{2+}, Hg^{2+}, Ag^{+}, etc. In CH_3OH/H_2O (90:10; v/v; HEPES=7.4) solvent system, all the examined cations showed negligible interfere with the detection of Cu^{2+}.

Therefore, absorption signal of probe **1** with negligible interference is a good indication for the presence of Cu^{2+} (**Figure 8**)

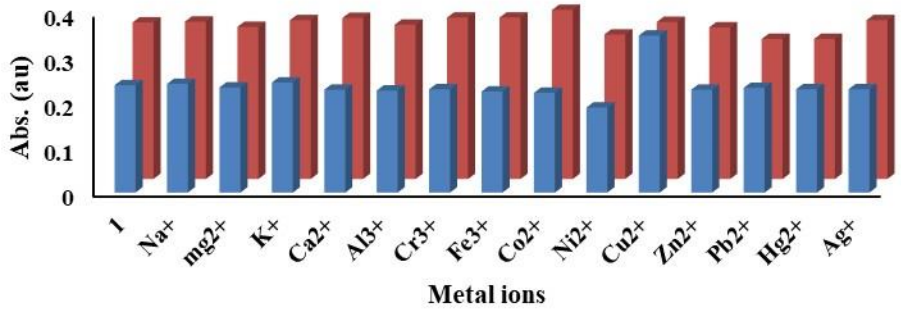

Figure 8. Relative absorbance intensity of probe **1** (10 μM) in CH_3CN/H_2O:9:1) with different competing metal ions in the absence and presence of Cu^{2+}, at λ = 450 nm, where blue bar represents the emission intensity change of probe **1** with different metal ions and red bars represents probe **1** with Cu^{2+} plus different relevant competing metal ions**.**

4.2.3 Effect of various cations on emission spectrum of probe 1:

Probe **1** (10 μM, CH_3OH/H_2O:9:1) on excitation at 420 nm showed no emission enhancement for other metal ions such as Na^+, Mg^{2+} , K^+, Al^{3+} , Cr^{3+}, Fe^{3+}, Co^{2+}, Ni^{2+}, Cu^{2+}, Zn^{2+} , Pd^{2+}, Hg^{2+}, Ag^+. However, the addition of Al^{3+} ions to the solution of probe **1** causes sudden emission enhancement at 515 nm (Figure **9**). On the other hand, the addition of various other ions did not show any significant change to the emission of probe **1**. On gradual addition of Al^{3+} (0-250 μM) to the

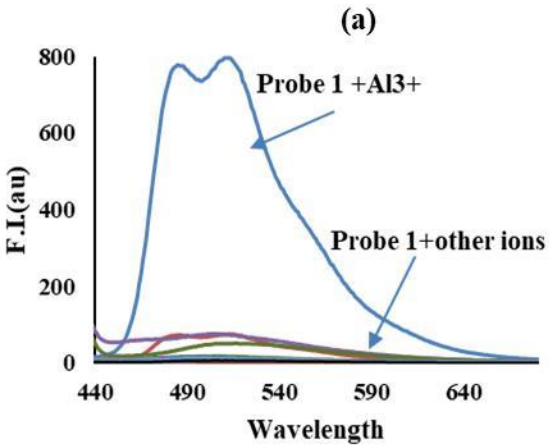

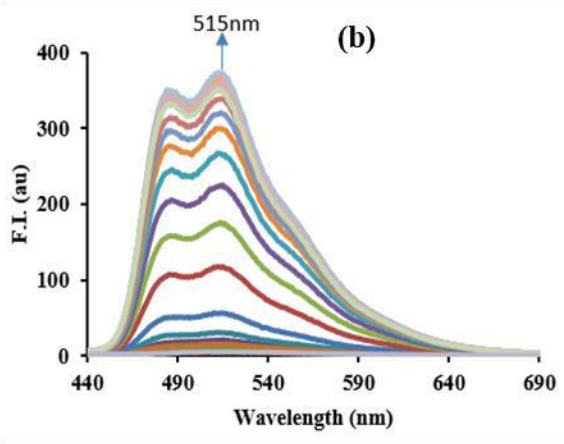

Figure 9. (a) Emission spectra of probe 1 (10 μM in CH_3OH/H_2O:9:1) in the absence and presence of various cations such as Na^+, Mg^{2+}, K^+, Al^{3+}, Cr^{3+}, Fe^{3+}, Co^{2+}, Ni^{2+}, Cu^{2+}, Zn^{2+}, Pd^{2+}, Hg^{2+}, Ag^+ (b) Effect of gradual addition of Al^{3+} to probe 1 (10 μM in CH_3OH/H_2O:9:1) on emission spectrum.

solution of probe **1**, a continuous growth in emission peak was observed at 515 nm. The emission at 515 nm vary from 1.9 to 345 indicating emission enhancement of ~125 fold. Thus, probe **1** can be used to estimate Al^{3+} with a detection limit of 3.2×10^{-7} M in CH_3OH/H_2O:9:1 solvent through emission "turn-on" approach (Figure **9**).

4.2.4 Practical Applicability of probe 1:

To evaluate the relative interference of another cations in Al^{3+} detection, (Figure **10**) the emission responses of probe **1** to Al^{3+} was measured in the presence of various metal ions such as Na^{+}, Mg^{2+}
, K^{+}, Al^{3+} , Cr^{3+}, Fe^{3+}, Co^{2+}, Ni^{2+}, Cu^{2+}, Zn^{2+} , Pd^{2+}, Hg^{2+}, Ag^{+}, etc. In CH_3OH/ H_2O:9:1 solvent system. All the examined cations showed negligible interfere with the detection of Al^{3+}. Therefore, emission signal of probe **1** with negligible interference is a good indication for the prime presence
of Al^{3+}.

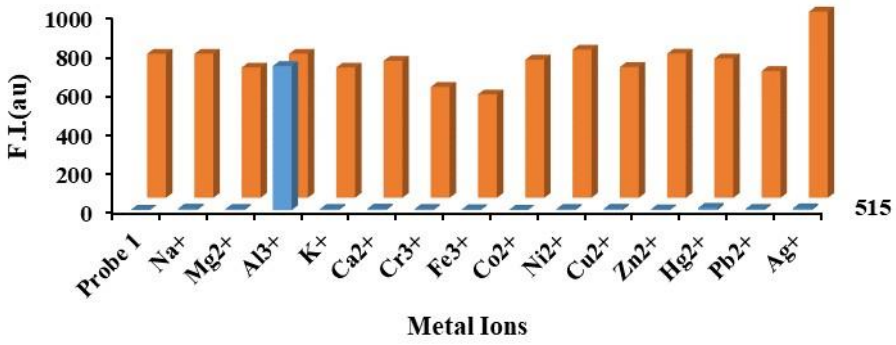

Figure 10. Relative emission intensity of probe **1** (10 μM) in CH_3OH/H_2O:9:1 (λex = 420 nm) with different competing metal ions in the absence and presence of Al^{3+} , at λ = 515 nm, where blue bar represents the emission intensity change of probe **1** with different cations and red bars represents probe **1** with Al^{3+} plus different relevant competing cations.

4.2.5 Job's plot analysis of Probe 1 towards Cu^{2+} and Al^{3+}:

To determine complexation behavior of probe **1** towards Cu^{2+} ion and Al^{3+}, Job′s Plot was drawn **(Figure 11).** A stock solution of the same concentration of probe **1** and Cu^{2+} and probe 1 and Al^{3+} was prepared of the order of 2.0×10^{-5} M in (CH_3OH/H_2O:9:1) solvent system for the Cu^{2+} and Al^{3+}. The emission of each case with equal volume but different probe analyte ratio was recorded. Job plots were drawn by plotting emission intensity vs X analyte (ΔI = change in intensity of the

emission spectrum during titration, Xanalyte is the mole fraction of analyte in each case) and found that there exists a 1:1 stoichiometry.

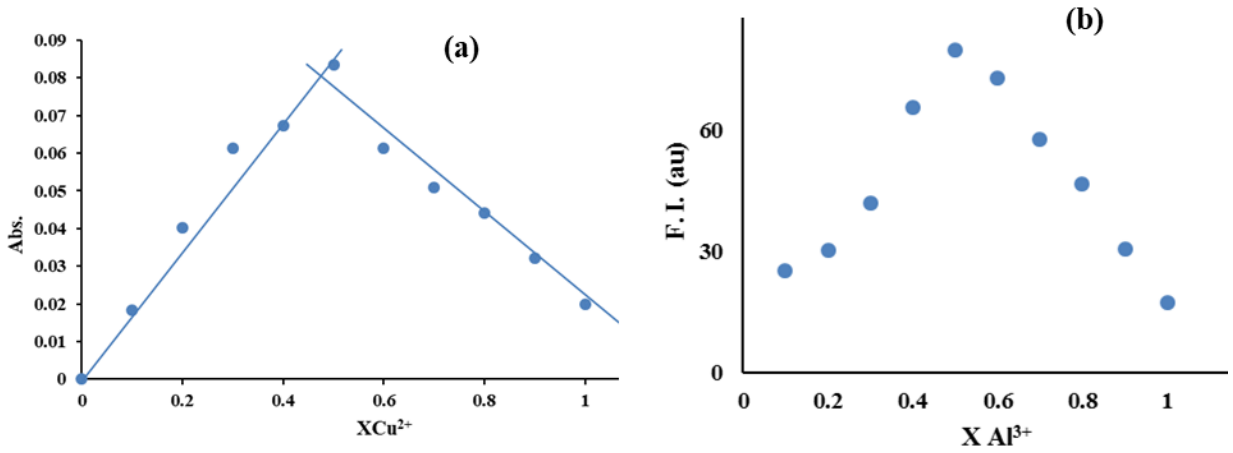

Figure 11. Job′s plot diagram of probe **1** with Cu^{2+} ions in $CH_3CN:H_2O$:9:1 (b) Job′s plot of probe **1** with Al^{3+} ions in $CH_3CN:H_2O$:9:1

4.2.6 Proposed Mechanism:

Job′s plot analysis revealed the stoichiometry of 1:1 for Probe **1** towards Cu^{2+} and Al^{3+}. Probe **1** has two OH units at naphthol and pyrimidine moiety, Schiff base nitrogen group, which could provide the binding sites for metal ions. A pictorial representation has been shown in Figure **12**.

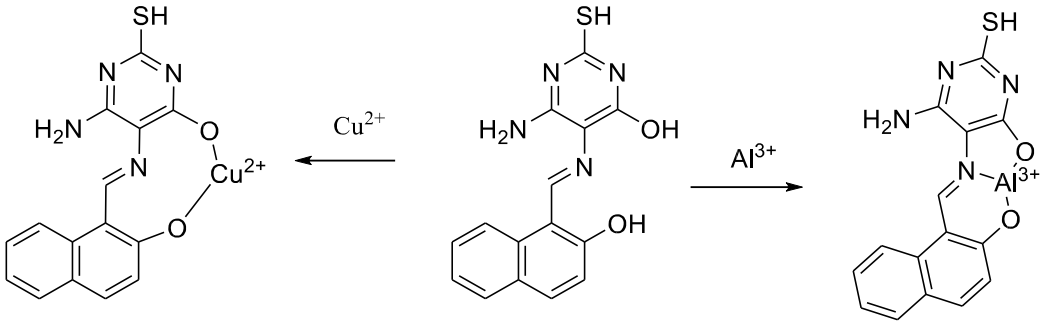

Figure 12. Proposed mechanism for Electrophilic attack of Al^{3+} and Cu^{2+} ion on Probe **1.**

4.2.7 Absorption Studies of probe 3 towards cations and anions:

The photo physical properties of probe **3** were measured through absorption and emission spectroscopy. (**Figure 13**) The absorption band of probe **3** showed maxima at 420 nm in CH_3CN/H2O:9:1. Further, the recognition behavior of the probe **3** toward various cations, such Na^+, Mg^{2+} , K^+, Al^{3+}, Cr^{3+}, Fe^{3+}, Co^{2+}, Ni^{2+}, Cu^{2+}, Zn^{2+}, Pd^{2+}, Hg^{2+}, Ag^+ and anions CN^-, SCN^-,

OAc^-, HSO_4^-, $H_2PO_4^-$, NO_3^-, F^-, Br^-, Cl^-, OCl^- was investigated by UV–visible and emission studies. Among different metal ions no significant changes has been observed for any of ions in

CH_3CN/H_2O (9:1; v/v; HEPES pH = 7.2) solvent system.

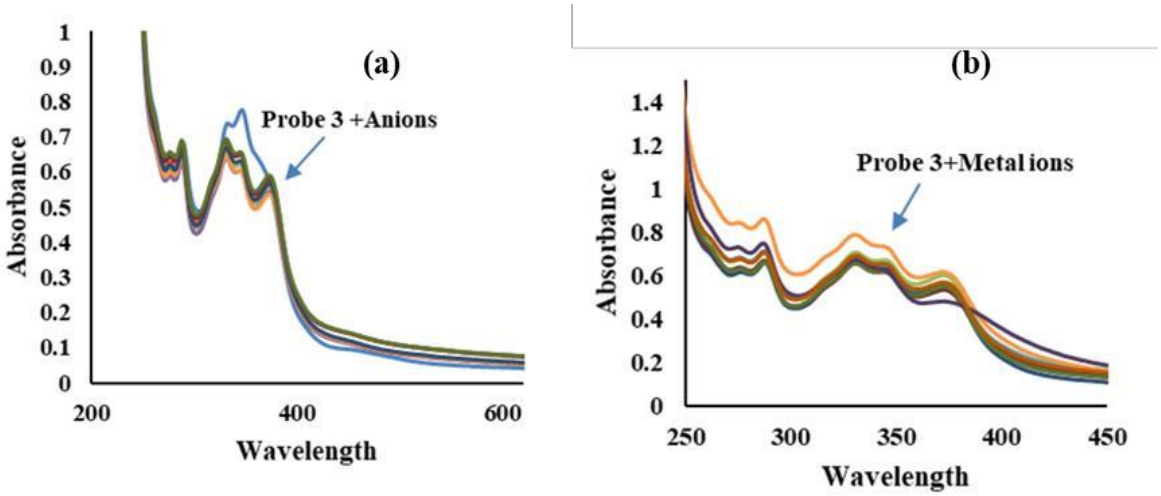

Figure 13. (a) UV–Visible spectra of probe **3** (10 µM in CH_3CN/H_2O::90:10) with absence and presence of different cations such as Na^+, Mg^{2+}, K^+, Al^{3+}, Cr^{3+}, Fe^{3+}, Co^{2+}, Ni^{2+}, Cu^{2+}, Zn^{2+}, Pd^{2+}, Hg^{2+}, Ag^+ ions . (b) a) UV-Visible spectra of probe **3** (10 µM in CH_3CN/H_2O::9:1) with absence and presence of different anions such CN^-, SCN^-, OAc^-
, HSO_4^-, $H_2PO_4^-$, NO_3^-, F^-, Br^-, Cl^-, OCl^- as ions.

4.2.8 Effect of Various anions on Probe 3:

The emission spectra of probe **3** (10 µM, CH_3CN/H_2O:9:1) showed emission maxima at 440 nm, so the probe exhibited very weak fluorescence (Figure **14**). On addition of various anions (CN^-, SCN^-, OAc^-, HSO_4^-, $H_2PO_4^-$, NO_3^-, F^-, Br^-, Cl^-, OCl^-), no significant change was observed except for OCl^- ion. On the addition of OCl^- ion, the probe **3** showed emission enhancement at 440 nm. On gradual addition of OCl^- (0-575 µM) to the solution of probe **3**, the emission peak at 440 nm was enhanced .The emission at 440 nm vary from 101 to 325 indicating emission enhancement of fold. Thus, probe **3** can be used to estimate OCl^- ion with a detection limit of 7.4×10^{-7} M in aqueous (CH_3CN/H_2O:9:1) solvent through "turn-on" emission approach.

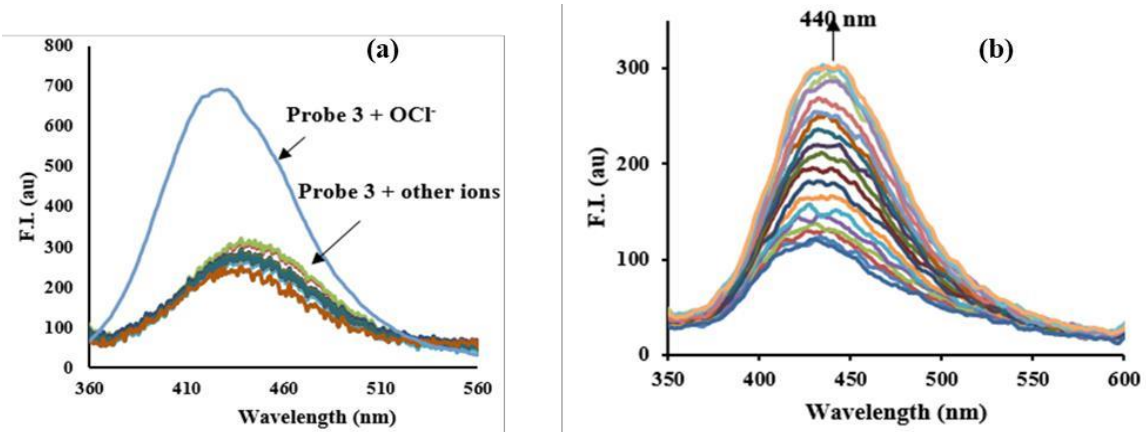

Figure 14. (a) Emission spectra of probe **3** (10 µM in CH_3CN/H_2O:9:1) in the absence and presence of different anions such as CN^-, SCN^-, OAc^-, HSO_4^-, $H_2PO_4^-$, NO_3^-, F^-, Br^-, Cl^-, OCl^- (b) Effect of incremental addition of OCl^- to probe **3** (10 µM, CH_3CN/H_2O::9:1) on emission spectrum.

4.2.9 Interferences of other anions:

To evaluate the relative interference of various anions in OCl^- detection, we measured the fluorescence responses of probe **3** towards OCl^- (Figure **15**). OCl^- was measured in the presence of another anions such as CN^-, SCN^-, OAc^-, HSO_4^-, $H_2PO_4^-$, NO_3^-, F^-, Br^-, Cl^-, OCl^- etc. In CH_3CN/H_2O:9:1 solvent system, all the examined anions showed negligible interfere with the detection of OCl^-. Therefore, turn-on fluorescence signal of probe **3** is a good indication for the

prime presence of OCl^-.

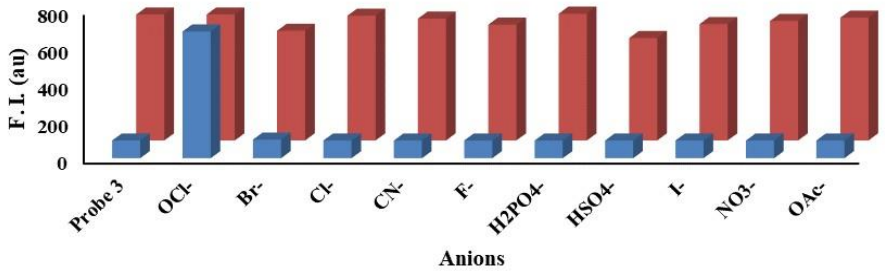

Figure 15. Relative emission intensity of probe **3** (10 µM) in CH_3CN/H_2O::9:1 (λex = 320 nm) with different competing anions in the absence and presence of OCl^-, at λ = 440 nm, the blue bar represents the emission intensity change of probe **3** with different anions and red bars represents probe **3** with OCl^- plus different relevant competing anions.

4.2.10 Proposed Mechanism:

The mechanism for recognition of OCl^- ions for probe **3** is under study, the exact mechanism could not be stated presently. The mass spectrometry, NMR titrations are under study.

Chapter 5 CONCLUSION

Probe **1** and Probe **3** were synthesized by incorporation of Schiff base and benzothiazole on naphthol as a core moiety, respectively. Probe **1** utilized as recognition for Cu^{2+} ions through absorption response and Al^{3+} ions through fluorometric response. On addition of Cu^{2+} ions **1** showed a redshift in absorption spectrum from 420 nm to 450 nm. On the other hand, introduction of Al^{3+} ions showed enhancement in fluorescence at 515 nm. Thus, probe **1** chemosensors exhibited *"turn-on"* on addition of Al^{3+} ion. On the other hand, probe **3** showed *"turn-on"* response for OCl^- ions at 440 nm on excitation at 320 nm. Thus, probe **1**, **3** exhibited *"turn-on"* responses for Al^{3+} and OCl^- ions respectively.

Chapter 6 REFERENCES

1. K. Velmurugan and R. Nandhakumar, *J. Lumin.*, 2015, **162**, 8-13.
2. J. Wu, W. Liu, J. Ge, H. Zhang and P. Wang, *Chem. Soc. Rev.*, 2011, **40**, 3483-3495.
3. D. Wu, A. C. Sedgwick, T. Gunnlaugsson, E. U. Akkaya, J. Yoon and T. D. James, *Chem. Soc. Rev.*, 2017, **46**, 7105-7123.
4. X. Chen, T. Pradhan, F. Wang, J. S. Kim and J. Yoon, *Chem. Rev.*, 2011, **112**, 1910-1956.
5. F. Wang, R. Nandhakumar, Y. Hu, D. Kim, K. M. Kim and J. Yoon, *J. Org. Chem.*, 2013, **78**, 11571-11576.
6. A. Akdeniz, T. Minami, S. Watanabe, M. Yokoyama, T. Ema and P. Anzenbacher, *Chem. Sci.*, 2016, **7**.
7. J. Y. Kwon, Y. J. Jang, Y. J. Lee, K. M. Kim, M. S. Seo, W. Nam and J. Yoon, *J. Am. Chem. Soc.*, 2005, **127**, 10107-10111.
8. J. M. Brunel, *Chem. Rev.*, 2007, **107**, PR1-PR45.
9. X. Liang, T. D. James and J. Zhao, *Tetrahedron*, 2008, **64**, 1309-1315.
10. R. Peng, L. Lin, X. Wu, X. Liu and X. Feng, *J. Org. Chem.*, 2013, **78**, 11602-11605.
11. N. Yadav and A. K. Singh, *Mater. Sci. Eng., C*, 2018, **90**, 468-475.
12. C. Chang, F. Wang, J. Qiang, Z. Zhang, Y. Chen, W. Zhang, Y. Wang and X. Chen, *Sens. Actuators, B*, 2017, **243**, 22-28.
13. J. Shi, Q. Li, X. Zhang, M. Peng, J. Qin and Z. Li, *Sens. Actuators, B*, 2010, **145**, 583-587.
14. Q.-S. Lu, L. Dong, J. Zhang, J. Li, L. Jiang, Y. Huang, S. Qin, C.-W. Hu and X.-Q. Yu, *Org. Lett.*, 2009, **11**, 669-672.
15. S.-Y. Jiao, L.-L. Peng, K. Li, Y.-M. Xie, M.-Z. Ao, X. Wang and X.-Q. Yu, *Analyst*, 2013, **138**, 5762-5768.
16. V. Luxami and S. Kumar, *RSC Advances*, 2012, **2**, 8734-8740.
17. J. Jiao, X. Liu, X. Mao, J. Li, Y. Cheng and C. Zhu, *New J. Chem.*, 2013, **37**, 317-322.
18. H.-L. Liu, Q.-L. Zhao, X.-L. Hou and L. Pu, *Chem. Commun.*, 2011, **47**, 3646-3648.
19. L. Yang, S. Qin, X. Su, F. Yang, J. You, C. Hu, R. Xie and J. Lan, *Org. Biomol. Chem.*, 2010, **8**, 339-348.
20. A. S. Gupta, K. Paul and V. Luxami, *Anal. Methods*, 2018, **10**, 983-990.
21. A. S. Gupta, G. Kumar, K. Paul and V. Luxami, *New J. Chem.*, 2018, **42**, 2491-2497.
22. M. Dong, Y.-M. Dong, T.-H. Ma, Y.-W. Wang and Y. Peng, *Inorg. Chim. Acta*, 2012, **381**, 137-142.
23. N. Gupta, D. Singhal and A. K. Singh, *New J. Chem.*, 2016, **40**, 641-650.
24. A. S. Gupta, G. Sharma, K. D. Paul and V. Luxami, *New J. Chem.*, 2018.
25. S. S. Mati, S. Chall, S. Konar, S. Rakshit and S. C. Bhattacharya, *Sens. Actuators, B*, 2014, **201**, 204-212.
26. N. Maurya and A. K. Singh, *New J. Chem.*, 2017, **41**, 4814-4819.
27. C. H. Min, S. Na, J. E. Shin, J. K. Kim, T. G. Jo and C. Kim, *New J. Chem.*, 2017, **41**, 3991-3999.

thesis

ORIGINALITY REPORT

11%	5%	8%	3%
SIMILARITY INDEX	INTERNET SOURCES	PUBLICATIONS	STUDENT PAPERS

PRIMARY SOURCES

1	Nidhi Singla, Venkata Srinu Bhadram, Chandrabhas Narayana, Papia Chowdhury. "White Light Generation by Carbonyl Based Indole Derivatives Due to Proton Transfer: An Efficient Fluorescence Sensor", The Journal of Physical Chemistry A, 2013 Publication	1%
2	www.beilstein-journals.org Internet Source	1%
3	riunet.upv.es Internet Source	1%
4	125.235.3.98 Internet Source	1%
5	Jiao, Shu-Yan, Ling-Ling Peng, Kun Li, Yong-Mei Xie, Mei-Zhen Ao, Xin Wang, and Xiao-Qi Yu. "A BINOL-based ratiometric fluorescent sensor for Zn2+ and in situ generated ensemble for selective recognition of histidine in aqueous solution", The Analyst, 2013. Publication	1%